Sains Malaysiana 55(7)(2026): 1148-1160
http://doi.org/10.17576/jsm-2026-5507-04

In vitro and *in silico* Investigation of Bioactive Compounds from *Arcangelisia flava* (L.) Merr. as Potential Antibacterial Agents

(Kajian *in vitro* dan *in silico* terhadap Sebatian Bioaktif daripada *Arcangelisia flava* (L.) Merr. sebagai Agen Antibakteria yang Berpotensi)

NENI FRIMAYANTI[1], IHSAN IKHTIARUDIN[1], JASRIL[2], LUKMAN LA BASY[3] & RUDI HENDRA[2,4,*]

[1]*Sekolah Tinggi Ilmu Farmasi Riau, Jalan Kamboja, Simpang Baru, Pekanbaru, 28293 Indonesia*
[2]*Department of Chemistry, Faculty of Mathematics and Natural Sciences, Universitas Riau, Pekanbaru, 28293 Indonesia*
[3]*Department of Pharmacy, STIKES Maluku Husada, Maluku, 97566 Indonesia*
[4]*Centre of Biological Innovation for Regenerative and Natural Applications, Universitas Riau, Pekanbaru, 28293 Indonesia*

Received: 6 February 2026/Accepted: 11 July 2026

ABSTRACT

The growing threat of antibiotic resistance has prompted the hunt for new antibacterial medicines derived from natural sources. This work examined four compounds isolated from *Arcangelisia flava* (L.) Merr. roots: palmatine (**1**), fibraurin (**2**), β-sitosterol (**3**), and daucosterol (**4**). Both *in vitro* and *in silico* methods were used to assess their antibacterial properties. The antibacterial activity was assessed against *Staphylococcus aureus, Bacillus subtilis, Vibrio alginolyticus,* and *Salmonella typhimurium* using the broth microdilution method, which determined the minimum inhibitory concentration (MIC) and minimum bactericidal concentration (MBC). Palmatine (**1**) and fibraurin (**2**) had modest action against Gram-positive bacteria, with MIC values of 37.5 µg/mL. However, β-sitosterol (**3**) and daucosterol (**4**) showed lesser inhibition. Docking against bacterial protein targets (PDB IDs: 2ZDQ and 1HNJ) found palmatine (1) had the highest binding affinity (−7.7980 and −7.5464 kcal/mol, respectively), generating numerous hydrogen bonds and hydrophobic interactions. Pharmacophore analysis identified critical structural features - aromatic rings and hydrogen bond donors/acceptors - that are linked to the observed antibacterial activities. Palmatine (**1**) and fibraurin (**2**) met drug-likeness criteria, but β-sitosterol (**3**) and daucosterol (**4**) had limited absorption and potential for toxicity. Overall, (**1**) and fibraurin (**2**) are intriguing lead candidates for antibacterial drug development, requiring additional *in vivo* testing and structural tweaking to improve efficacy.

Keywords: ADMET analysis; antibacterial activity; *Arcangelisia flava*; molecular docking; pharmacophore modeling

ABSTRAK

Ancaman peningkatan rintangan antibiotik telah mendorong usaha mencari agen antibakteria baharu yang berasaskan sumber semula jadi. Penyelidikan ini mengkaji empat sebatian yang diasingkan daripada akar *Arcangelisia flava* (L.) Merr., iaitu palmatin (**1**), fibraurin (**2**), β-sitosterol (**3**) dan daucosterol (**4**). Kaedah *in vitro* dan *in silico* digunakan untuk menilai sifat antibakteria sebatian tersebut. Aktiviti antibakteria diuji terhadap *Staphylococcus aureus*, *Bacillus subtilis*, *Vibrio alginolyticus* dan *Salmonella typhimurium* menggunakan kaedah pencairan cecair skala kecil bagi menentukan kepekatan perencatan minimum (MIC) dan kepekatan minimum bakterisid (MBC). Palmatin (**1**) dan fibraurin (**2**) menunjukkan aktiviti sederhana terhadap bakteria Gram-positif dengan nilai MIC sebanyak 37.5 µg/mL, manakala β-sitosterol (**3**) dan daucosterol (**4**) memperlihatkan perencatan yang lebih rendah. Kajian pengikatan secara pendokan terhadap sasaran protein bakteria (PDB ID: 2ZDQ dan 1HNJ) menunjukkan bahawa palmatin (**1**) memiliki pertalian pengikatan tertinggi (masing-masing −7.7980 dan −7.5464 kcal/mol) disertai pembentukan ikatan hidrogen dan interaksi hidrofobik yang signifikan. Analisis farmakofor mengenal pasti ciri struktur kritikal - gelang aromatik serta penderma/penerima ikatan hidrogen - yang berkaitan dengan aktiviti antibakteria yang diperhatikan. Palmatin (**1**) dan fibraurin (**2**) turut memenuhi kriteria seakan ubat, manakala β-sitosterol (**3**) dan daucosterol (**4**) menunjukkan penyerapan yang terhad serta potensi ketoksikan. Secara keseluruhan, palmatin (**1**) dan fibraurin (**2**) merupakan calon awal yang menarik untuk pembangunan ubat antibakteria, namun memerlukan ujian *in vivo* tambahan dan pengubahsuaian struktur bagi meningkatkan keberkesanan.

Kata kunci: Aktiviti antibakteria; analisis ADMET; *Arcangelisia flava*; pemodelan farmakofor; pengikatan molekul

INTRODUCTION

The global rise in antibiotic resistance has become a major public health challenge, highlighting the urgent need to discover new antibacterial agents, particularly those derived from natural products. Medicinal plants encompass various classes of phytochemicals, including alkaloids, flavonoids, terpenoids, and saponins, which are well-documented for their antimicrobial properties via mechanisms such as membrane disruption, essential enzyme inhibition, and metabolic pathway interference (Abdallah et al. 2023; Caioni et al. 2024). Endophytic bacteria linked to these plants have been proven to be abundant sources of bioactive metabolites, frequently generating chemicals that are structurally similar to or even more powerful than those of their host species (Adeleke & Babalola 2021). Among these types of natural products, alkaloids are particularly distinguished for their extensive antibacterial activity, chemical stability, and comparatively low tendency to induce bacterial resistance (Álvarez-Martínez et al. 2025). Notwithstanding their promising pharmacological potential, constraints such as low yields, chemical unpredictability, and difficulties in large-scale manufacture persist in obstructing their wider therapeuticutilization.

Arcangelisia flava (L.) Merr., a climbing species prevalent in Southeast Asia, has historically been utilized in traditional medicine for the treatment of febrile and viral ailments. Prior phytochemical and pharmacological studies have demonstrated that this species encompasses various bioactive secondary metabolites, including berberine, 6-hydroxyfibraurin, and fibleucin, which display antibacterial and anti-inflammatory properties, likely by disrupting bacterial protein synthesis and cell wall biosynthesis. Ethanolic extracts of *A. flava* have proven anti-inflammatory activities through the suppression of interleukin-1β, while endophytic bacteria isolated from this species have shown antibacterial activity against pathogenic strains (Masrukhin et al. 2022; Pratama et al. 2023). Rudi et al. (2024) recently showed the antifungal activity of palmatine (**1**) and fibraurin (**2**) against Candida species, underscoring the extensive antibacterial potential of *A. flava* metabolites.

Despite these promising findings, the antibacterial activities of several compounds isolated from *A. flava* remain poorly understood. Prior research has predominantly concentrated on crude extracts, restricted chemical classes, or singular-target computational forecasts, leading to an inadequate comprehension of the molecular pathways that govern the antibacterial properties of certain isolated metabolites. Specifically, there is an absence of comprehensive investigations concurrently assessing the *in vitro* antibacterial efficacy, binding interactions with bacterial molecular targets, and pharmacokinetic and safety profiles of *A. flava* metabolites.

This study examines four compounds - palmatine (**1**), fibraurin (**2**), β-sitosterol (**3**), and daucosterol (**4**) - extracted from the roots of *A. flava* to fill the existing information gap. An extensive experimental and computational methodology was utilized, incorporating *in vitro* antibacterial testing, molecular docking, pharmacophore modeling, and absorption-distribution-metabolism-excretion-toxicity (ADMET) profiling. This multi-tiered methodology assesses their antibacterial efficacy while also clarifying their structural characteristics, binding interactions, and drug-like properties. This integrative assessment seeks to identify the most promising antibacterial lead candidates from the extracted metabolites and offer mechanistic insights to facilitate future optimization and development against bacterial pathogens, including resistant strains.

MATERIALS AND METHODS

GENERAL EXPERIMENTAL PROCEDURE

The isolated compounds - palmatine (**1**), fibraurin (**2**), β-sitosterol (**3**), and daucosterol (**4**) - were obtained from the active fraction of *Arcangelisia flava* roots following the procedure described by Rudi et al. (2024). Standard Mueller–Hinton broth (MHB) and Mueller–Hinton agar (MHA) were purchased from Oxoid (Basingstoke, UK). Chloramphenicol (≥98% purity), used as the positive control, was obtained from Sigma-Aldrich (St. Louis, MO, USA). Dimethyl sulfoxide (DMSO) was purchased from Merck (Darmstadt, Germany) and used as the solvent for compound preparation at a final concentration not exceeding 1% (v/v) in antibacterial assays. All other chemicals and reagents were of analytical grade and used without further purification.

ANTIBACTERIAL ACTIVITY

The minimum inhibitory concentration (MIC) and minimum bactericidal concentration (MBC) of the tested compounds were determined using the method described by Hilwan et al. (2024) and Monika et al. (2023). A 96-well microtiter plate to determine the MIC, adhering to the conventional broth microdilution method, while the MBC was evaluated using Mueller Hinton agar (MHA) plates with analogous protocols. Bacterial suspensions were produced at a concentration of 10^6 colony-forming units (CFU) per milliliter prior to initiation.

For the MIC assay, we introduced 100 µL of the extract stock solution, achieving a final concentration of 250 µg/mL, into the wells and conducted a two-fold serial dilution utilizing 100 µL of the bacterial inoculum in Mueller-Hinton broth. The dilution was executed from column 12 to column 3, with column 12 containing the greatest extract concentration and column 3 the lowest. Column 1 served as negative control, comprising solely the growing media, whereas column 2 functioned as the

positive control, containing both bacteria and medium without the extract. Following a 24-h incubation of the plates at 37 °C, we examined them for observable bacterial growth. The MIC was determined as the minimum concentration at which bacterial growth was absent.

To determine the MBC, samples from each well were transferred onto MHA plates and incubated for 24 h at 37 °C. The MBC was defined as the lowest concentration at which no bacterial colonies grew on the agar surface. Chloramphenicol served as the positive control, and all tests were performed in triplicate to ensure reliable and consistent results.

MOLECULAR DOCKING

The molecular structures of the ligands and chloramphenicol (positive control) were sourced from the PubChem database and manually created using the MOE Builder module. The MMFF94x force field was employed to calculate the energy minimization of the ligands. Figure 1 illustrates the molecular structure of these ligands.

Molecular docking was performed using the Molecular Operating Environment (MOE, Chemical Computing Group, version 2022.0901) to investigate ligand–protein interactions and evaluate the binding affinities of the selected compounds. The three-dimensional structure of the target protein was acquired from the RCSB Protein Data Bank (https://www.rcsb.org). This work utilized two protein targets to address specific cellular activities. The initial target (PDB ID: 2ZDQ) was focused on disrupting cell wall structures. The secondary target (PDB ID: 1HNJ) sought to inhibit protein synthesis. Protein preparation commenced with the purification of its structure, entailing

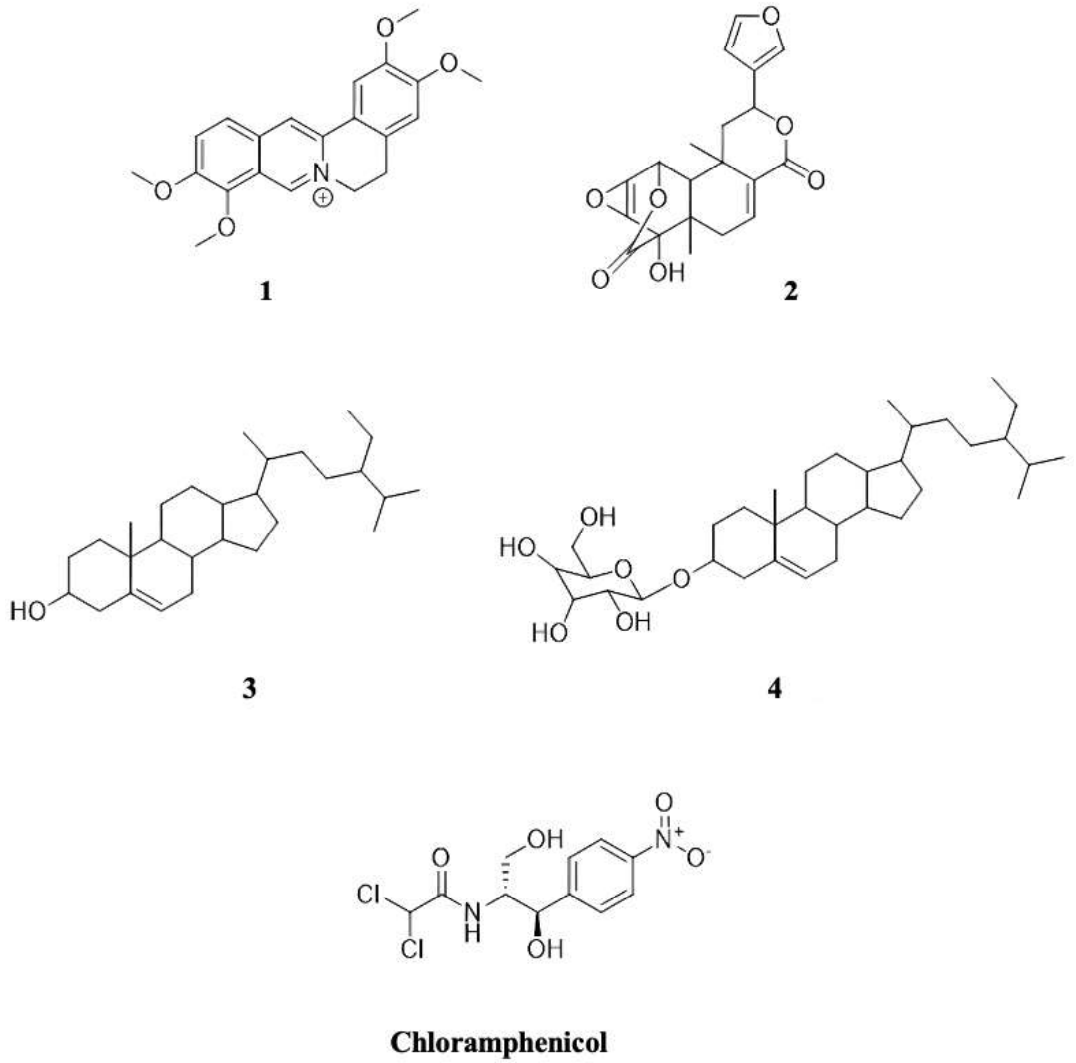

FIGURE 1. Molecular structure of chlorampenicol (positive control) and palmatine (**1**), fibraurin (**2**) β-sitosterol (**3**), and daucasterol (**4**)

the elimination of water molecules, existing ligands, and co-crystallized ions with MOE's Structure Preparation tools. The protonation states were modified, and partial charges were allocated utilizing the Protonate 3D capability. The protein structure underwent additional refinement via energy reduction employing the CHARMM27 force field until the RMS gradient decreased to 0.01 kcal/mol/Å² (Owoloye et al. 2022).

The protein's active site was determined utilizing the Site Finder program. The ligand, created and stored in an MDB file, was chosen for docking. The docking process commenced by designating the active site to a dummy atom using the dock option. The docking configuration employed the triangle matcher technique for positioning, with the adjustability configured to be firm. The placement and refinement processes were set to produce 100 initial postures, succeeded by 50 refinement iterations. Energy computations were executed with the CHARMM27 force field, with the docking grid size established at 26 × 26 × 22 units along the x, y, and z axes, respectively. The optimal docking results were chosen according to multiple criteria, including minimal binding free energy, advantageous RMSD values, and robust binding scores, with particular emphasis on poses exhibiting binding interactions akin to those of the positive control (Neni et al. 2025).

PHARMACOPHORE

The protein's active site was determined utilizing the Site Finder program. The ligand, created and stored in an MDB file, was chosen for docking. The docking process commenced by designating the active site to a dummy atom using the dock option. The docking configuration employed the triangle matcher technique for positioning, with the adjustability configured to be firm. The placement and refining procedures were established to produce 100 initial postures, succeeded by 50 refinement iterations. Energy computations were conducted with the CHARMM27 force field, with the docking grid size established at 26 × 26 × 22 units along the x, y, and z axes, respectively. The optimal docking results were chosen according to multiple criteria, including minimal binding free energy, advantageous RMSD values, and robust binding scores, with particular emphasis on poses exhibiting binding interactions akin to those of the positive control (Ira et al. 2024).

ADMET AND DRUG-LIKENESS

The pharmacokinetic characteristics and drug-likeness of the chosen compounds were assessed utilizing ADMETlab 3.0 (https://admetlab3.scbdd.com/), a sophisticated online platform created by the Shanghai Institute of Materia Medica. Each compound was transformed into its canonical SMILES format and submitted to the ADMETlab 3.0 system for evaluation. This platform was utilized to forecast the essential ADMET (absorption, distribution, metabolism, excretion, and toxicity) attributes. The assessment concentrated on factors including human intestinal absorption (HIA), Caco-2 cell permeability, blood-brain barrier (BBB) penetration, and interactions with P-glycoprotein (P-gp), encompassing both substrate and inhibitor capabilities. Metabolic stability was evaluated by estimating the inhibition of cytochrome P450 (CYP450) enzymes, including the principal isoforms CYP3A4, CYP2D6, CYP2C9, CYP2C19, and CYP1A2. The drug-likeness was further evaluated using recognized criteria, such as Lipinski's Rule of Five and the bioavailability score (Lipinski et al. 2001). The investigation also encompassed toxicity hazards, focusing on hERG channel blockage, AMES mutagenicity, hepatotoxicity, and acute oral toxicity of the drugs. This *in silico* assessment yielded a thorough comprehension of the pharmacokinetic properties and safety profiles of the compounds, facilitating the identification of those with the greatest promise as medication candidates.

RESULTS AND DISCUSSION

ANTIBACTERIAL ACTIVITY

The antibacterial efficacy of the examined substances was evaluated against four bacterial strains: *S. aureus, B. subtilis, V. alginolyticus*, and *S. typhimurium*. The microdilution approach was employed to evaluate their efficacy by diluting the compounds and obtaining their MIC and MBC. Table 1 illustrates the results for MIC and MBC.

Compounds **1** and **2** showed modest antibacterial activity, particularly against Gram-positive bacteria such as *S. aureus* and *B. subtilis*, as determined by MIC and MBC assays. Their activity against Gram-negative bacteria, including *S. typhimurium*, was comparatively lower, likely due to the presence of protective outer membranes that hinder compound penetration (Leus et al. 2023). Based on the MBC/MIC ratio criterion, both compounds generally exhibited bactericidal effects (MBC/MIC < 4) against *S. aureus*, while displaying predominantly bacteriostatic activity (MBC/MIC > 4) against other tested strains, particularly Gram-negative bacteria. This indicates that while these compounds may effectively kill certain Gram-positive bacteria, their primary mode of action against most Gram-negative bacteria is growth inhibition rather than direct killing, consistent with the observed structural barriers and potential efflux mechanisms limiting intracellular accumulation (Whittle et al. 2021).

Compound **3** exhibited the lowest antibacterial efficacy, with MIC values between 37.5 and 75 µg/mL and MBC values over 150 µg/mL for most bacterial strains, signifying minimal bactericidal potency.

TABLE 1. Minimum inhibition concentration and minimum bactericidal concentration of compounds **1-4**

Compound	*S. aureus*		*B. subtillis*		*V. algynolyticus*		*S. typhimurium*	
	MIC	MBC	MIC	MBC	MIC	MBC	MIC	MBC
1	37.5	75	37.5	150	37.5	150	150	>150
2	37.5	150	37.5	150	37.5	150	150	>150
3	75	>150	75	>150	37.5	>150	>150	>150
4	37.5	>150	37.5	150	37.5	>150	37.5	>150
Chloramphenicol	18.75	37.5	18.75	37.5	18.75	37.5	18.75	37.5

Concentration in µg/mL

Compound **4** exhibited MIC values of 37.5 µg/mL against three bacterial strains; nevertheless, dosages over 150 µg/mL were generally necessary to achieve bactericidal effects. Conversely, chloramphenicol consistently exhibited the highest antibacterial efficacy against all evaluated bacteria, with low MIC (18.75 µg/mL) and MBC (37.5 µg/mL) values. These results indicate that while Compounds **1** and **2** have moderate antibacterial properties, they are inferior to chloramphenicol, the most effective drug in this study.

MOLECULAR DOCKING

Molecular docking is a commonly used computational approach that helps to predict how a compound or ligand fits into the binding site of a target protein. Docking was performed with two protein targets, and the docking results for PDB ID 2ZDQ and 1HNJ are presented in Tables 2 and 3, respectively.

Molecular docking was conducted to examine the interactions of the isolated chemicals with two bacterial targets: MurD (PDB ID: 2ZDQ) and TyrRS (PDB ID: 1HNJ). These chemicals exhibited unique binding affinities for both proteins. Among the evaluated compounds, palmatine (1) consistently exhibited the most robust binding, with binding free energies of −7.7980 kcal/mol for MurD and −7.5464 kcal/mol for TyrRS, accompanied by RMSD values below 2 Å, indicating dependable docking conformations. The binding affinities were comparable to or marginally superior to those of chloramphenicol. Conversely, fibraurin (**2**) demonstrated considerable binding, whereas β-sitosterol (**3**) and daucosterol (**4**) displayed less advantageous interaction patterns, although compound **4** had a more acceptable docking score. The observed interactions, such as hydrogen bonds, hydrophobic contacts, and van der Waals forces, facilitated the stability of the ligand–protein complexes (He et al. 2023; Neni et al. 2024).

The docking outcomes were predominantly aligned with the *in vitro* antibacterial evaluation results. Because the antibacterial activities were experimentally confirmed by MIC and MBC assays, the molecular docking analysis was intended to provide a mechanistic interpretation of the observed biological activity rather than to establish enzyme inhibition directly. Palmatine, which exhibited the lowest MIC values against the studied microorganisms, also demonstrated the most robust binding affinity for both MurD and TyrRS. The planar protoberberine scaffold facilitated advantageous hydrogen bonding and hydrophobic interactions with essential active-site residues, offering a credible structural rationale for its enhanced antibacterial efficacy. Fibraurin exhibited a comparable, albeit less persistent, binding method, presumably because of the reduced number of hydrogen-bonding groups, whereas β-sitosterol and daucosterol mostly engaged through hydrophobic interactions owing to their substantial steroidal configurations.

Figures 2 and 3 show the characteristic binding mechanisms of the evaluated compounds at the active sites of MurD and TyrRS, respectively. Palmatine exhibited the most advantageous orientation in both enzymes, penetrating deeply into the catalytic regions and forming several stabilizing contacts. In contrast, fibraurin displayed a reduced number of stabilizing connections, whereas β-sitosterol and daucosterol assumed less advantageous conformations, presumably diminishing their capacity for efficient interaction with the catalytic areas. The structural discrepancies align with the variances in the docking scores and antibacterial efficacy noted among the drugs.

Despite daucosterol exhibiting comparatively advantageous docking scores, its antibacterial efficacy was inferior to that of palmatine and fibraurin, indicating that binding affinity alone does not dictate the biological activity. Molecular size, glycosylation, polarity, and membrane permeability are expected to affect the antibacterial activity. Consequently, the docking study should be considered as further mechanistic evidence that bolsters the experimental antibacterial findings, rather than as conclusive proof of enzyme inhibition. The integrated *in vitro* and *in silico* results identified palmatine as the most promising lead drug among the isolated metabolites. Further confirmation

through biochemical assays and molecular dynamics simulations would provide a better understanding of the mechanism of action of this compound.

PHARMACOPHORE

Pharmacophore modelling was used to elucidate the essential chemical attributes potentially contributing to the antibacterial efficacy of the four discovered drugs. This work displayed functional groups that influence a compound's interaction with bacterial target proteins, including hydrophobic regions, aromatic rings, and hydrogen bond donors/acceptors (Kouassi et al. 2021). The pharmacophore visualization for the four drugs is illustrated in Figure 4.

Palmatine (**1**) demonstrated the most advantageous pharmacophore profile, characterized by a harmonious configuration of aromatic rings alongside hydrogen bond donor and acceptor functionalities. These characteristics promote π–π stacking and hydrogen bonding interactions with bacterial target proteins, which is consistent with its enhanced docking efficacy and antibacterial properties. Fibraurin (**2**) had a comparable structural framework although contained less hydrogen-bonding

TABLE 2. Docking results for PDB ID 2ZDQ

Compound	Binding free energy (kcal/mol)	RMSD	H bond	Hydrophobic	van der Walls	The others interaction	Binding factor
chloramphenicol	-7.3186	1.3055	Arg268,Asn281, Lys153, Glu189	Ser159, Tyr223, Lys228, Lys116	Glu13, Asp270, Glu197, Glu282	Gly158, Ser160, Asn284, Phe222, Phe272, Phe151, Ile163	19
1	-7.7980	1.0237	**Arg268, Asn284, Glu197**	**Lys153, Lys116, Lys228**	Glu199, **Asp270,** Glu13, **Glu282**	Thr292, Gly288, Ser293, Tyr229, Met294, Pro287, **Gly158, Ser159, Tyr223, Ser160, Asn281, Ile163, Phe272, Phe222**	16
2	-6.7481	1.2014	Ala191, Leu192, **Lys228**	**Lys116, Lys153,** Lys190	**Asp270, Glu197, Glu282, Glu189**	Tyr218, **Tyr223, Ile163, Phe272, Phe151,** Val131, **Phe222, Asn281, Ser160**	14
3	-7.0505	1.2443	**Phe151**	**Lys228, Lys153, Lys116, Arg268**	**Glu13, Glu197, Asp270, Glu282**	Met294, **Ser159,** Ser293, Pro287, Tyr229, **Gly158,** Gly288, **Phe222,** Ser160, **Tyr223, Phe272,** Tyr218, Val195, **Asn284, Ile163, Asn281,** Thr157	17
4	-7.5220	1.5718	-	Leu192, **Lys228, Arg268,** Lys190, Arg165, **Lys153**	**Glu282,** Glu199, **Asp270**, **Glu197, Glu13**	**Asn281, Tyr223, Asn284, Phe272,** Tyr218, Ala191, Ser193, Val195, Pro221, **Phe151, Phe222, Ile163, Ser160, Ser159, Gly158,** Ser293, Thr292, Gly288, His82, Met294, Val16, Tyr229	17

TABLE 3. Docking results for PDB ID 1HNJ

Compound	Binding free energy (kcal/mol)	RMSD	H bond	hydrophobic	van der Walls	The others interaction	Binding factor
chloramphenicol	-7.4209	1.3984	Cys112	Arg36	-	Phe304, Ile250, Gly209, Asn274, Val212, Met207, His244, Ala246, Leu189, Asn210, Ile156, Ala216, Asn247, Phe213, Thr37, Trp32,	18
1	-7.5464	1.1342	**Ala246**	**Arg36**	**-**	**His244,** Gly305, **Cys112, Phe304, Phe213, Asn274, Leu189, Ile156, Met207,** Phe157, **Gly209,** Gly152, **Asn210, Trp32, Ile250, Val212, Asn247**	16
2	-6.1119	0.8759	**Met207**	**Arg36,** Arg249	-	**Phe304, Leu189, Ala246, Asn274, Ile250, Asn247, Ile156, Thr37,** Gly152, **Trp32, Phe213, Asn210, Val212, Gly209,** Gly309	15
3	-6.3632	1.7824	Arg249	**Arg36,** Arg151	Asp150	**Asn247, Gly209, Met207, Asn210, Phe213,** Thr149, **Trp32,** Gly152	7
4	-7.3772	1.1287	Arg196	Ala83	-	Asn193, Ala86, Thr84, His85, Thr81, Ala109, Thr80, Gly306, Gly307, **Leu189,** Gly186, Thr190	1

characteristics, indicating a heightened reliance on hydrophobic and van der Waals interactions. This disparity likely accounts for its diminished antibacterial efficacy compared to palmatine.

Conversely, β-sitosterol (**3**) and daucosterol (**4**) demonstrated pharmacophore patterns characterized primarily by hydrophobic attributes. The inflexible steroidal framework of β-sitosterol restricts specific polar interactions with protein active sites, whereas the large glycosyl group of daucosterol may hinder its structural compatibility inside the binding pocket, despite its low hydrogen-bonding capacity. These traits align with their comparatively diminished antibacterial efficacy and fewer advantageous contact patterns identified in docking analysis (Madhulata et al. 2016; Pan, Wang & Bryant 2013).

Pharmacophore analysis corroborated the structure–activity link identified in both experimental and molecular docking studies. Compounds exhibiting an optimal blend of aromatic, hydrophobic, and hydrogen-bonding characteristics, notably palmatine, displayed enhanced antibacterial efficacy and greater binding affinity for the chosen bacterial targets. In contrast, substances characterized by primarily hydrophobic pharmacophoric attributes or enhanced steric bulk show less biological activity. These findings further substantiate palmatine as the most promising lead molecule among the identified metabolites and provide valuable structural information for the future optimization of antibacterial medicines.

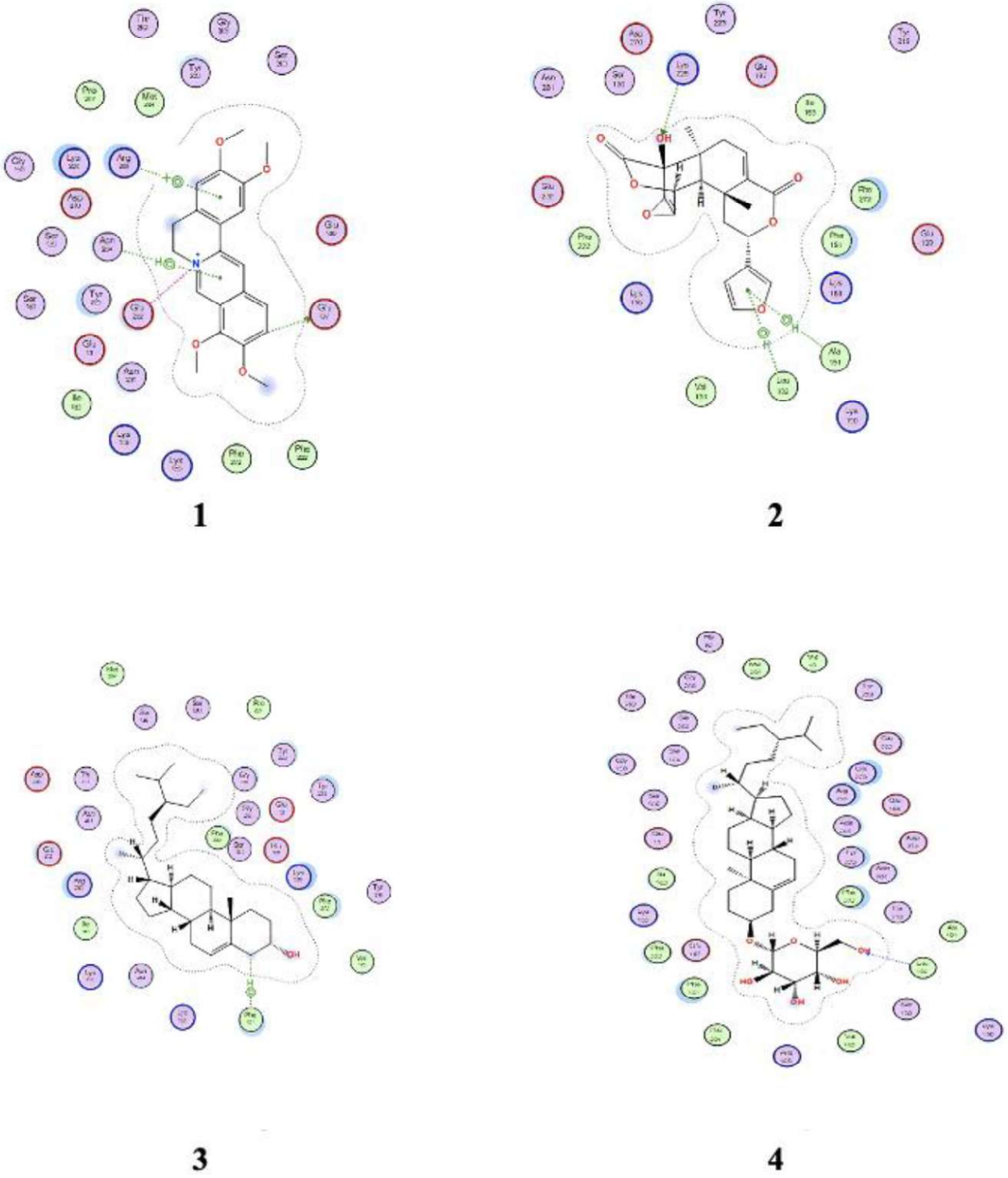

FIGURE 2. Spatial arrangement of (**1**) palmatine (**2**) fibraurin (**3**) β-sitosterol, and (**4**) daucasterol with protein target (PDB ID 2ZDQ)

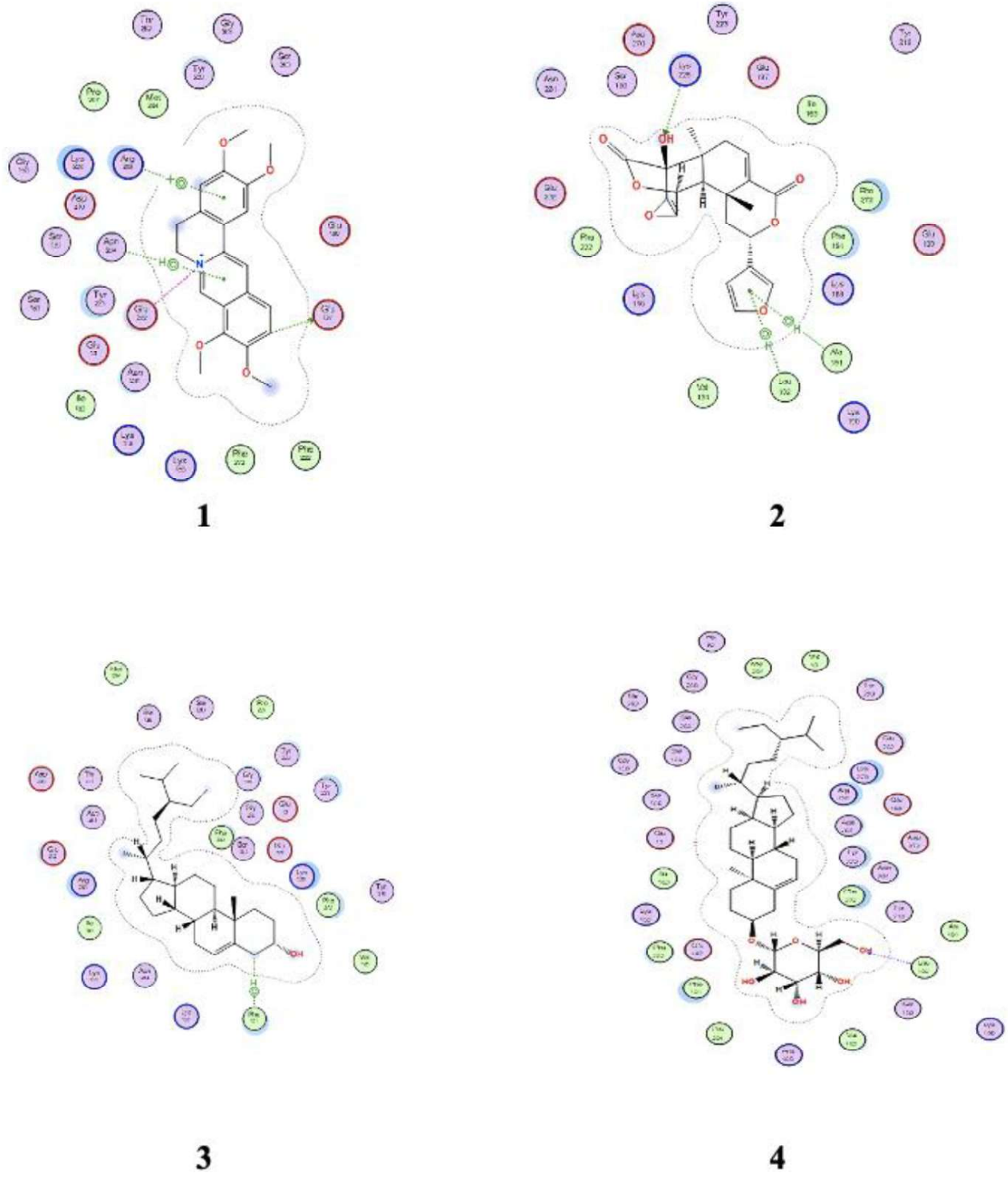

FIGURE 3. Spatial arrangement of (**1**) palmatine (**2**) fibraurin (**3**) β-sitosterol, and (**4**) daucasterol with protein target (PDB ID 1HNJ)

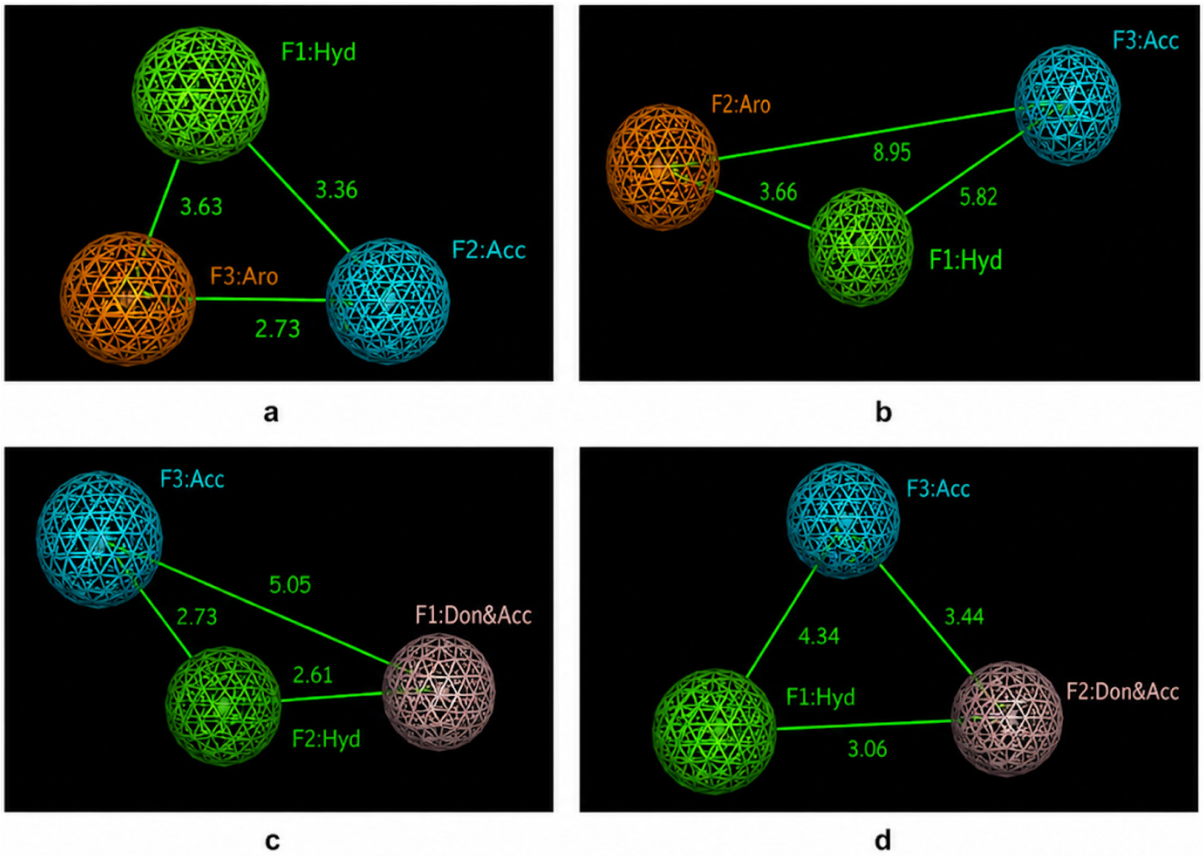

FIGURE 4. Pharmacophore for (a) palmatine (b) fibraurin (c) β-sitosterol, and (d) daucosterol

ADMET AND DRUG-LIKENESS

The ADMET evaluation provided an extensive analysis of the pharmacokinetic properties and safety considerations of the five tested drugs, as well as the positive control (Table 4). All compounds, with the exception of compound **4**, satisfied the criteria established by Lipinski's Rule of Five, indicating favorable prospects for oral bioavailability (Lipinski et al. 1997). Compound **4** surpassed the advised thresholds for both molecular weight and LogP, suggesting potential difficulties in permeability and absorption. Within the group, compounds **1** and **2** distinguished themselves by possessing the most advantageous physicochemical profiles, characterized by optimal molecular weight, satisfactory hydrogen bond properties, and TPSA values that align with drug-like criteria (Daina, Michielin & Zoete 2017).

Predictions indicated that all drugs exhibited low human intestinal absorption (HIA), remaining below the 0.3 threshold (Syahri et al. 2023). Nonetheless, compounds **2** and **3** exhibited comparatively superior membrane permeability according to Caco-2 assay results. Notably, compound **1** did not function as a substrate or inhibitor of P-glycoprotein, but the other compounds exhibited differing levels of interaction, potentially affecting drug transport and resistance. Compounds **2** and **3** exhibited elevated projected oral bioavailability (F20% and F30%), indicating an enhanced likelihood of achieving effective systemic concentrations.

In terms of distribution, compound **1** exhibited plasma protein binding (PPB) below 90%, indicating a higher fraction may stay unbound and pharmacologically active in circulation. Compound **2** demonstrated the highest capability for traversing the blood-brain barrier (BBB), whilst the other compounds were less probable to infiltrate the central nervous system. The volume of distribution values for all compounds were within acceptable ranges, with compounds **2** and **3** exhibiting enhanced diffusion throughout human tissues.

Metabolic models indicated that the chemicals typically had a minimal risk of blocking key cytochrome P450 enzymes, hence diminishing the probability of substantial drug-drug interactions. Compound **2** was identified as a substrate for multiple CYP isoforms, specifically CYP1A2, CYP2C19, CYP2D6, and CYP3A4, suggesting it may experience significant hepatic metabolism. The elimination, half-life, and clearance values for compounds **1**, **2**, and **3** were within the anticipated therapeutic range. Compound **4**, conversely, exhibited decreased clearance, perhaps resulting in extended systemic exposure. Table 4 presents the ADMET and drug-likeness data.

TABLE 4. ADMET and drug-likeness

Parameter		Positive control	1	2	3	4
Drug-likeness *Lipinski*		Yes	Yes	Yes	Yes	No
Molecular weight (g/mol)	≤ 500	**322.01**	**352.4**	**372.37**	**414.39**	574.42
H-bond acceptor	≤ 10	**7**	**4**	**7**	**1**	**6**
H-bond donor	≤ 5	**3**	**0**	**1**	**1**	**4**
LogP	≤ 5	**0.79**	**3.785**	**2.414**	8.025	6.175
TPSA (Å²)	≤ 140	**112.7**	**40.80**	**98.50**	**20.23**	**99.38**
Human Intestinal Absorption (HIA)	> 0.3	0.012	0.016	0.012	0.002	0.258
Caco-2 permeability (log cm/s)	> -5.15	**-5.454**	**-4.764**	**-5.249**	**-4.679**	-4.857
P-glycoprotein inhibitor	A = < 0.5	**0.001**	0.982	0.923	0.972	0.975
P-glycoprotein substrate	A = < 0.5	**0.027**	**0.011**	**0.009**	**0.092**	0.771
$F_{20\%}$	> 0.3	0.001	**0.864**	**0.801**	**0.889**	**0.933**
$F_{30\%}$	> 0.3	0.0	**0.573**	**0.967**	0.054	0.137
D *(Distribution) Plasma Protein Binding (PBB) (%)*	< 90%	**61.57**	98.823	90.704	93.38	**86.19**
Blood-Brain Barrier Penetration (BBB) (cm/s)	> 0.1 cm/s	0.06	0.014	**0.71**	**0.136**	0.009
Volume distribution (L/kg)	0.04-20 L/kg	0.674	2.754	2.424	1.484	1.183
Fraction unbound (Fu) (%)	> 10%	**36.31**	2.851	11.628	1.296	1.335
CYP1A2 inhibitor		**0.032**	**0.177**	**0.116**	**0.095**	**0.015**
CYP1A2 substrate		**0.105**	0.967	**0.487**	0.526	**0.398**
CYP2C19 inhibitor		**0.041**	**0.026**	**0.36**	**0.143**	**0.017**
CYP2C19 substrate		0.837	0.92	0.509	0.923	0.771
CYP209 inhibitor	< 0.5	**0.007**	**0.006**	**0.176**	**0.208**	**0.11**
CYP209 substrate		**0.42**	0.826	**0.031**	**0.131**	**0.038**
CYP2D6 inhibitor		**0.003**	**0.241**	**0.046**	**0.142**	**0.017**
CYP2D6 substrate		**0.164**	**0.936**	**0.138**	**0.334**	**0.151**
CYP3A4 inhibitor		**0.026**	**0.036**	0.936	0.538	0.507
CYP3A4 substrate		**0.208**	0.723	**0.294**	0.731	0.585
Half time (t1/2)	1-4 h	**0.441**	**0.039**	**0.103**	**0.049**	**0.113**
Clearance (mL/min/kg)	5-15	**5.116**	11.748	13.094	7.21	**1.426**
Human hepatotoxicity (H-HT)	< 0.5	**0.053**	0.543	**0.223**	**0.131**	**0.189**
hERG blockers	< 0.5	**0.073**	**0.254**	**0.039**	0.875	**0.469**
Rat oral acute toxicity	< 0.5	**0.04**	**0.197**	0.958	**0.003**	**0.209**
AMES toxicity	< 0.5	**0.438**	**0.073**	**0.326**	**0.002**	**0.027**
Drug Induced Liver Injury (DILI)	< 0.5	**0.055**	0.614	**0.223**	0.551	**0.053**
Carcinogencity	< 0.5	**0.081**	**0.155**	0.89	**0.12**	**0.089**

Text in bold indicates that parameter is fulfilled

ADMET predictions further elucidated the drug-likeness and pharmacokinetic feasibility of the compounds. Palmatine and fibraurin adhered to many drug-likeness criteria, including Lipinski's Rule of Five, and demonstrated anticipated favorable oral bioavailability, sufficient distribution, and acceptable metabolic stability. Palmatine's anticipated advantageous plasma protein binding characteristics and minimal danger of P-glycoprotein-mediated efflux indicate an increased likelihood of sustaining effective systemic concentrations. Fibraurin, although advantageous in absorption, exhibited anticipated blood–brain barrier permeability and an extensive CYP450 substrate profile, potentially affecting clearance rates and the likelihood of drug–drug interactions. Conversely, β-sitosterol and daucosterol demonstrated inadequate anticipated intestinal absorption, elevated lipophilicity (LogP), and potential safety issues, such as hepatotoxicity and hERG channel blockage, hence constraining their therapeutic potential.

The broader implications of these results extend to antibacterial drug discovery, particularly with respect to overcoming the intrinsic resistance mechanisms of Gram-negative bacteria. The limited activity against Gram-negative strains observed in this work emphasizes the challenges posed by outer membrane impermeability and efflux pump activity. Future optimization strategies may include enhancing lipophilicity–polarity balance, reducing molecular weight, or incorporating functional groups that promote membrane traversal. Additionally, coupling alkaloid cores with permeabilizing agents or nanoparticle delivery systems may further improve antibacterial efficacy, especially against problematic Gram-negative pathogens.

The study's limitations comprise a restricted bacterial panel that excluded multidrug-resistant clinical isolates; dependence on docking as the exclusive computational validation without subsequent molecular dynamics simulations or free energy perturbation calculations; and the lack of *in vivo* pharmacokinetic, toxicity, or efficacy studies to validate the predicted ADMET profiles. Future efforts should encompass broadening the antibacterial spectrum examined to incorporate resistant clinical pathogens, incorporating biochemical assays to confirm enzyme inhibition, and utilizing molecular dynamics to evaluate binding stability under physiological settings. Furthermore, semi-synthetic alterations of palmatine and fibraurin, informed by structure-activity relationship (SAR) insights, may improve Gram-negative efficacy by adjusting polarity, diminishing efflux vulnerability or integrating membrane-permeabilizing components. Thorough *in vivo* ADME/Tox investigations, together with efficacy assessments in animal infection models, will be crucial for progressing these drugs to preclinical development.

CONCLUSIONS

This research showed that palmatine and fibraurin extracted from *Arcangelisia flava* displayed moderate antibacterial efficacy, especially against Gram-positive bacteria, as validated by *in vitro* MIC and MBC assays. Molecular docking, pharmacophore analysis, and ADMET prediction substantiate these experimental results by offering credible mechanistic and pharmacokinetic insights into their antibacterial efficacy. Computational analyses should be considered supplementary evidence rather than conclusive validation of the postulated mechanisms of action. Despite both compounds exhibiting lower activity than chloramphenicol, their advantageous structural features and pharmaceutical qualities indicate their potential as lead compounds for subsequent optimizations. Subsequent research utilizing enzyme inhibition assays, molecular dynamics simulations, and *in vivo* assessments is necessary to corroborate the postulated mechanisms and facilitate the progression of these compounds in the development of antibacterial medications.

ACKNOWLEDGEMENTS

We express our gratitude for the support received from the Ministry of Education, Culture, Research and Technology of the Republic of Indonesia for research funding via Grant No. 144/C3/DT.05,00/PL-MULTITAHUN LANJUTAN/2026.

REFERENCES

Abdallah, E.M., Alhatlani, B.Y., Menezes, R.d.P. & Martins, C.H.G. 2023. Back to nature: Medicinal plants as promising sources for antibacterial drugs in the post-antibiotic era. *Plants* 12(17): 3077.

Adeleke, B.S. & Babalola, O.O. 2021. Pharmacological potential of fungal endophytes associated with medicinal plants: A review. *Journal of Fungi* 7(2): 147.

Álvarez-Martínez, F.J., Díaz-Puertas, R., Barrajón-Catalán, E. & Micol, V. 2025. Plant-derived natural products for the treatment of bacterial infections. In *Natural Products as Sources of Novel Drugs*, edited by Wainwright, C.L., Schini-Kerth, V.B. Springer, Cham. pp. 265-293.

Caioni, G., Reyes, C.P., Laurenti, D., Chiaradia, C., Dainese, E., Mattioli, R., Di Risola, D., Santavicca, E. & Francioso, A. 2024. Biochemistry and future perspectives of antibiotic resistance: An eye on active natural products. *Antibiotics* 13(11): 1071.

Daina, A., Michielin, O. & Zoete, V. 2017. SwissADME: A free web tool to evaluate pharmacokinetics, drug-likeness and medicinal chemistry friendliness of small molecules. *Scientific Reports* 7(1): 42717.

He, Q., Liu, C., Wang, X., Rong, K., Zhu, M., Duan, L., Zheng, P. & Mi, Y. 2023. Exploring the mechanism of curcumin in the treatment of colon cancer based on network pharmacology and molecular docking. *Frontiers in Pharmacology* 14: 1102581.

Hilwan Yuda Teruna, Rohimatul Khodijah, Neni Frimayanti & Rudi Hendra. 2024. Phytochemicals from *Pyrrosia longifolia* (Burm. f.) C.V. Morton with antibacterial activity. *Research in Pharmaceutical Sciences* 19(6): 712-728. doi: 10.4103/RPS.RPS_151_23

Ira Arundina, Neni Frimayanti, Meircurius Dwi Condro Surboyo, Theresia Indah Budhy & Benni Iskandar. 2024. 6-octadecenoic and oleic acid in liquid smoke rice husk showed COVID-19 inhibitor properties. *Advances in Pharmacological and Pharmaceutical Sciences* 2024: 8105595.

Kouassi, K.A.R., Ganiyou, A., Benié, A., Koné, M.G-R., Nobel, N.K., Bohoussou, K.V. & Coulibaly, W.K. 2021. Identification of potential C-kit protein kinase inhibitors associated with human liver cancer: Atom-based 3D-QSAR modeling, pharmacophores-based virtual screening and molecular docking studies. *Am. J. Pharmacol. Sci.* 9(1): 1-29.

Leus, I.V., Adamiak, J., Chandar, B., Bonifay, V., Zhao, S., Walker, S.S., Squadroni, B., Balibar, C.J., Kinarivala, N. & Standke, L.C. 2023. Functional diversity of Gram-negative permeability barriers reflected in antibacterial activities and intracellular accumulation of antibiotics. *Antimicrobial Agents and Chemotherapy* 67(2): e01377-22.

Lipinski, C.A., Lombardo, F., Dominy, B.W. & Feeney, P.J. 1997. Experimental and computational approaches to estimate solubility and permeability in drug discovery and development settings. *Advanced Drug Delivery Reviews* 23(1-3): 3-25.

Madhulata Kumari, Subhash Chandra, Neeraj Tiwari & Naidu Subbarao. 2016. 3D QSAR, pharmacophore and molecular docking studies of known inhibitors and designing of novel inhibitors for M18 aspartyl aminopeptidase of *Plasmodium falciparum*. *BMC Structural Biology* 16(1): 12.

Monika Kerry Army, Rohimatul Khodijah, Yuli Haryani, Hilwan Yuda Teruna & Rudi Hendra. 2023. Antibacterial *in vitro* screening of *Helminthostachys zeylanica* (L.) Hook. root extracts. *Journal of Pharmacy & Pharmacognosy Research* 11(2): 291-296. doi: https://doi.org/10.56499/jppres22.1540_11.2.291

Neni Frimayanti, Abdi Wira Septama, Hilwan Yuda Teruna & Eldiza Puji Rahmi. 2025. *In silico* investigation of artocarpin, cycloarotcarpin, artocarpanone, and cyanomaclurin for dengue virus inhibitor DEN2 NS2B/NS3 serine protease. *J. Pharm. Pharmacogn. Res.* 13(1): 193-202.

Neni Frimayanti, Ihsan Ikhtiarudin, Rahma Dona, Rahul Oktarizal & Aprilia Cindy Nurfatimah. 2024. Exploring substituted tetrazoloquinazoline: biological activities, molecular docking analysis, and anti-breast cancer MCF7/HER2 effects. *Advances in Pharmacological and Pharmaceutical Sciences* 2024(1): 6952142.

Owoloye, A.J., Ligali, F.C., Enejoh, O.A., Musa, A.Z., Aina, O., Idowu, E.T. & Oyebola, K.M. 2022. Molecular docking, simulation and binding free energy analysis of small molecules as Pf HT1 inhibitors. *PLoS ONE* 17(8): e0268269.

Pan, Y., Wang, Y. & Bryant, S.H. 2013. Pharmacophore and 3D-QSAR characterization of 6-arylquinazolin-4-amines as Cdc2-like kinase 4 (Clk4) and dual specificity tyrosine-phosphorylation-regulated kinase 1A (Dyrk1A) inhibitors. *Journal of Chemical Information and Modeling* 53(4): 938-947.

Rizki Rahmadi Pratama, Irawati Sholikhah, Ram Kumar Sahu & Retno Widyowati. 2023. Phytochemical compounds identification from 70% ethanol extract of *Arcangelesia flava* (L.) Merr. stems using LC-MS/MS and *in-silico* molecular docking approach as inhibitor interleukin-1β. *Pharmacognosy Journal* 15(4): 528-534. doi: http://dx.doi.org/10.5530/pj.2023.15.114

Rudi Hendra, Aulia Agustha, Neni Frimayanti, Rizky Abdulah & Hilwan Yuda Teruna. 2024. Antifungal potential of secondary metabolites derived from *Arcangelisia flava* (L.) Merr.: An analysis of *in silico* enzymatic inhibition and *in vitro* efficacy against *Candida* species. *Molecules* 29(10): 2373. doi: https://doi.org/10.3390/molecules29102373

Sipriyadi, Masrukhin, Risky Hadi Wibowo, Welly Darwis, Salprima Yudha, Ismu Purnaningsih & Resli Siboro. 2022. Potential antimicrobe producer of endophytic bacteria from yellow root plant (*Arcangelisia flava* (l.)) originated from Enggano Island. *International Journal of Microbiology* 2022: 6435202.

Syahri, J., R. Hilma, N. Nurlaili, M.K. Sari, N. Frimayanti, A.M. Ali, and J. latip. 2023. "Synthesis, Antimalarial Activities of Secondary Amine-Substituted Eugenol Compounds against Plasmodium falciparum and in silico Molecular Docking Analysis." *Sains Malaysiana* 52 (12):3463-3474.

Whittle, E.E., McNeil, H.E., Trampari, E., Webber, M., Overton, T.W. & Blair, J.M.A. 2021. Efflux impacts intracellular accumulation only in actively growing bacterial cells. *MBio* 12(5): 10.1128/mbio.02608-21.

*Corresponding author; email: rudi.hendra@lecturer.unri.ac.id